Applied Thermal Engineering 219 (2023) 119616

Contents lists available at ScienceDirect

Applied Thermal Engineering

journal homepage: www.elsevier.com/locate/ate

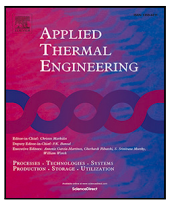

Research Paper

# Fast Bayesian inference for inverse heat conduction problem using polynomial chaos and Karhunen–Loeve expansions

Sufia Khatoon [a], Jyoti Phirani [b], Supreet Singh Bahga [a,*]

[a] Department of Mechanical Engineering, Indian Institute of Technology, Delhi, 110016, India
[b] Department of Civil and Environmental Engineering, University of Strathclyde, Glasgow, G1 1XJ, UK

ARTICLE INFO

*Keywords:*
Inverse heat conduction
Bayesian inference
Polynomial chaos expansions
Karhunen–Loeve expansion

ABSTRACT

We present a fast Bayesian inference framework for solving inverse heat conduction problems (IHCP) for the estimation of boundary heat flux. The framework leverages the polynomial chaos expansions (PCEs) for generating computationally efficient and statistically equivalent surrogate model of the computationally expensive forward model and dimensionality reduction based on Karhunen–Loeve (K–L) expansion. We demonstrate the potential of this approach using three model problems to estimate heat flux in inverse heat conduction models. We represent the heat flux using K–L expansion to reduce the high dimensionality of the heat flux and compute the posterior probability distribution of the heat flux using the temperature measurements. The first inverse problem involves the estimation of time–varying heat flux in a one–dimensional slab using transient temperature measurements. The second problem involves the estimation of the unknown time–dependent heat flux of the disc in a realistic axisymmetric disc brake system. The third problem involves the estimation of the surface heat flux on a sounding rocket having a realistic three–dimensional geometry of the rocket module used in actual flight tests. We further obtain the inverse solution by computing the expectation of the distribution and demonstrate that this approach becomes orders of magnitude more efficient when we use the PCE surrogate model instead of the direct forward model for comparable accuracy. The numerical results show that this framework overcomes the drawback of high computational cost of Markov chain Monte Carlo (MCMC) without compromising on solution accuracy. The combination of PC–based surrogate modeling and K–L based dimensionality reduction leads to over 2000–fold speed up of numerical solution of IHCP.

## 1. Introduction

A variety of physical phenomena can be described by forward mathematical models, which predict measurable quantities based on the governing equations, initial and boundary conditions, and the values of various model parameters. On the other hand, the inverse problems involve predicting these model parameters, boundary conditions, and the initial conditions from a set of observations. Inverse problems can be classified into two categories: (i) inverse problems that involve the design of engineering products, and (ii) those that come up in identifying physical processes. Inverse problems associated with engineering design involve figuring out the features of an engineering unit's design to achieve desired performance characteristics. Inverse problems of the second class involve the estimation of model parameters, such as the boundary conditions, thermophysical properties, initial conditions, or source terms. The latter class of inverse problems are usually part of experimental research, which involves figuring out the input of the experiment which caused the measured output.

In this paper we focus on the inverse heat conduction problem (IHCP) which involves the estimation of the unknown boundary heat flux or the thermophysical properties of the medium using temperature measurements. IHCPs for boundary heat flux estimation find application in various fields of science and engineering, including space technology [1,2], manufacturing process control [3], quenching hot metals or cooling down power electronics [4], aerospace and nuclear engineering [5], and medical diagnostics [6]. Such inverse problems involving the estimation of boundary conditions, such as the heat flux, can be solved either by a parameter or function estimation approach. They can be reduced to estimating a small number of parameters if some information is known about the functional form of the unknown boundary condition. However, with no prior knowledge of the unknown boundary condition's functional form, the inverse problem can be viewed as a function estimation technique in the space of functions with infinite dimensions [3].

* Corresponding author.
*E-mail address:* bahga@mech.iitd.ac.in (S.S. Bahga).

https://doi.org/10.1016/j.applthermaleng.2022.119616
Received 20 June 2022; Received in revised form 10 October 2022; Accepted 3 November 2022
Available online 13 November 2022

## Nomenclature

### Abbreviations

| | |
|---|---|
| 1-D | One-dimensional |
| 2-D | Two-dimensional |
| 3-D | Three-dimensional |
| BI | Bayesian inference |
| IHCP | Inverse heat conduction problem |
| K-L | Karhunen–Loeve |
| MCMC | Markov chain Monte Carlo |
| PCE | Polynomial chaos expansions |

### Greek symbols

| | |
|---|---|
| $\alpha$ | Scale parameter |
| $\alpha^*$ | Probability ratio |
| $\beta$ | Shape parameter |
| $\mu$ | Mean |
| $\Omega$ | Physical domain |
| $\Psi$ | Basis functions of the PCE |
| $\psi$ | One-dimensional hermite polynomials |
| $\rho$ | Density |
| $\sigma$ | Standard deviation of the measurement noise |
| $\tau$ | Correlation time |
| $\theta$ | Hyperparameter |
| $\xi$ | Stochastic dimension |
| $\lambda_k$ | Eigen values |
| $\phi_k$ | Eigen functions |
| $\pi_e$ | Probability density of measurement error |

### Other symbols

| | |
|---|---|
| $\boldsymbol{n}$ | Unit normal vector |
| $\boldsymbol{T}$ | Predicted values of temperature |
| $\boldsymbol{T}_{obs}$ | Observed temperature |
| $\boldsymbol{Z}$ | Vector of discretized heat flux |
| $\varphi_i$ | Probability density of $i$th component of measurement error |
| $c_k$ | K-L modes |
| $c_p$ | Specific heat capacity |
| $e$ | Measurements error |
| $G$ | Forward model |
| $h$ | Heat transfer coefficient |
| $k$ | Thermal conductivity |
| $N$ | Number of simulations |
| $n$ | Number of terms |
| $p$ | Order of polynomial |
| $q$ | Heat flux |
| $T$ | Temperature |
| $t$ | Time |
| $T_0$ | Initial temperature |
| $T_\infty$ | Ambient temperature |
| $w$ | Weight of quadrature points |
| $x, y, z, r$ | Coordinates |

The IHCPs are mathematically classified as ill-posed and their solutions are generally obtained numerically by reformulating them into an approximate well-posed problem. The various methods to solve IHCP can be classified into deterministic and stochastic methods. The deterministic methods try to find the solution to inverse problems without explicitly assuming any probabilistic model for the model parameters or for the errors in observed data. A direct way to determine the solution using a deterministic approach is the least squares method by finding the mismatch between observed data and the forward model. Moreover, regularization methods have been developed to impose well-posedness on the inverse problems. Various deterministic techniques, such as generalized or weighted least squares, $L_P$ norm solution [7], conjugate-gradient method [8,9], Levenberg–Marquardt method [3,10–12], golden section search method [13], decentralized fuzzy inference method [14,15], iterative regularization methods [11] have been developed for parameter and function estimations in inverse heat conduction problems. These deterministic methods are easy to implement and predict single values of model parameters through optimization to minimize the difference between measurement data and model prediction [16]. However, these methods do not provide higher-order statistics of the parameter estimates. More details on the deterministic methods are reviewed by Alifanov [2] and Ozisik et al. [3].

Stochastic methods for solving inverse problems model the uncertainties in model parameters with appropriate probability distributions and predict their estimated values. Genetic algorithms [17], particle swarm optimization [18], simulated annealing [19], and ensemble Kalman filter [20] are some types of stochastic methods that have been successfully applied to solve inverse heat transfer problems, allowing for the recovery of the thermophysical properties of a system [14,15]. Most of these stochastic methods are based on the Bayesian inference (BI) approach. The BI approach incorporates the known information regarding the unknown model parameters by starting with a prior belief of the model parameters in terms of a prior probability distribution. The uncertainty of the model parameters is propagated into the predictions of the final model. Finally, by comparing the measured data and the model predictions, the belief in model parameters is updated using the Bayes' rule [21]. This yields a posterior probability distribution of the model parameters and is in contrast to the deterministic methods, which provide single best-estimated values of the unknown model parameters. The BI framework also helps to quantify the uncertainty in the model parameters and shows a reduction in the uncertainty after incorporating the measured data with the prior belief. Moreover, BI also regularizes the ill-posedness of IHCP through regularization by the prior distribution.

The BI framework being a probabilistic approach does not give a single value of the estimated parameters but gives a probability distribution. The BI method requires efficient sampling strategies to sample the posterior distribution which is generally non-Gaussian for high dimensional problems [22]. The standard sampling method to sample the posterior distribution is based on the Markov chain Monte Carlo (MCMC) method. Sampling of the posterior distribution using MCMC sampling yields the mean, mode, and other higher-order moments of the given problem. The exploration of the posterior distribution of the unknown parameters using MCMC requires repeated evaluation of the forward model which can be computationally expensive for high-dimensional and complex heat conduction problems. The computational cost of these forward evaluations becomes prohibitive for Monte Carlo simulations generally requiring $10^5$–$10^6$ samples [23]. The previous studies on the use of BI for solving IHCP, such as those by Wang and Zabaras [23], Koutsourelakis [24], Parthasarathy and Balaji [25], and Cao et al. [26] all rely on this computationally expensive approach.

Various stochastic methods such as EnKF [20] and Gaussian processes [27] have been developed to overcome the limitation of high computational cost of MCMC. These methods are based on simplifying assumptions of Gaussian prior and posterior distributions. In this paper, we present an alternative method of accelerating BI without making any assumptions on the prior and posterior. This paper presents a formulation designed to accelerate evaluation of the posterior using a surrogate model based on polynomial chaos expansions (PCEs). PCE is

a way of representing a random variable in the form of an infinite series with a sequence of orthogonal polynomials as basis functions [28]. The polynomials are functions of another simpler random variable and the type of random variable decides the choice of orthogonal polynomials. The selection of polynomial basis is based on their orthogonality with respect to the probability density function of the simpler random variable. The surrogate models are represented by the series of orthogonal polynomials with respect to the distributions of the model parameters. The PCE representation of the model predictions also defines the uncertainty that is propagated through the forward model with a stochastic method. The forward uncertainty propagation yields a polynomial approximation of the forward model over the support of the prior. This approximation gives a reduced-dimensionality form of the forward model which serves as a surrogate to obtain the posterior, which is explored with MCMC.

To achieve further speedup in solving IHCP for boundary heat flux estimation using BI, we represent the uncertain heat flux profile using the Karhunen–Loeve (K-L) expansions. The K-L expansions represent random fields into a linear combination of orthogonal basis functions and random variables as coefficients or modes in the form of an infinite series [29]. The problem then transforms to the prediction of the unknown modes of the truncated K-L expansion using the BI approach. The use of K-L expansion provides the necessary regularization to determine continuous heat flux from finite data. Moreover, representation of heat flux in terms of K-L expansions reduce the inverse problem to the determination of a few coefficients as opposed to the estimation of time-varying heat flux at many discrete time instances. We show that the combination of K-L representation of uncertain heat flux along with PCE-based surrogate model yields a computationally efficient approach for solving complex IHCPs.

In the current work, we describe the BI framework based on PCE and K-L expansion to estimate unknown heat flux in inverse heat conduction problems. We begin by presenting the deterministic equations for modeling the forward heat conduction problem. Next, we describe the Bayesian inference methodology to solve IHCP. After that, we provide a brief overview of K-L expansion for dimensionality reduction of the forward model to solve the inverse problem using MCMC sampling. Following that, we represent the unknown heat flux using K-L expansion and transform the problem to the prediction of the unknown K-L modes using the BI approach. We then present the fast BI framework using the PCE-based surrogate model. Thereafter, we present results for estimating the heat flux in a 1-D slab, a realistic problem of heat flux estimation in a 2-D disc brake system, and the estimation of surface heat flux in a 3-D sounding rocket system based on the realistic geometry of the rocket module used in actual flight tests. We validate the framework for different heat flux profiles and compare the accuracy of posterior estimates and the efficiency of the method.

## 2. Methodology

In this section, we discuss the Bayesian inference approach using the PCE surrogate for estimating unknown transient boundary heat flux in heat conduction problem. We begin by discussing the basic governing equations which are used to solve a forward heat conduction problem. Then, we present the application of the Bayesian inference method for the inverse heat conduction problem, followed by a discussion on K-L expansion for dimensionality reduction of the unknown heat flux. Next, we discuss their application along with PCE surrogate to propagate uncertainty and accelerate the Bayesian inference method. We show the application of the method to three different IHCPs of varying complexity, which we discuss in detail in Section 3.

### 2.1. Problem formulation and governing equations for the forward problem

We consider transient heat conduction in a homogeneous medium without internal heat sources shown schematically in Fig. 1. The physical domain of the model problem is represented by $\Omega$. The known boundary conditions include the temperature $T_g(x,t)$ on $\Gamma_g$, the heat flux $q_h$ on $\Gamma_h$ and the heat transfer coefficient $h$ and temperature $T_i$ on $\Gamma_i$ ($\Gamma_g \cup \Gamma_h \cup \Gamma_i \cup \Gamma_0 = \Gamma$). The time-varying temperature in the medium is described by:

$$\rho c_p \frac{\partial T}{\partial t} = \nabla \cdot (k \nabla T), \quad \text{in} \quad \Omega, \quad t \in [0, t_{max}], \tag{1}$$

$$T(\boldsymbol{x}, t) = T_g(x,t), \quad \text{on} \quad \Gamma_g, \quad t \in [0, t_{max}], \tag{2}$$

$$-k \frac{\partial T(\boldsymbol{x},t)}{\partial \boldsymbol{n}} = q_h(x,t), \quad \text{on} \quad \Gamma_h, \quad t \in [0, t_{max}], \tag{3}$$

$$-k \frac{\partial T(\boldsymbol{x},t)}{\partial \boldsymbol{n}} = h \Delta T, \quad \text{on} \quad \Gamma_i, \quad t \in [0, t_{max}], \tag{4}$$

$$-k \frac{\partial T(\boldsymbol{x},t)}{\partial \boldsymbol{n}} = q_0(x,t) \quad \text{on} \quad \Gamma_0, \quad t \in [0, t_{max}], \tag{5}$$

$$T(\boldsymbol{x}, 0) = T_0(\boldsymbol{x}) \quad \text{in} \quad \Omega, \tag{6}$$

where $\rho$, $c_p$ and $k$ are the density, heat capacity and thermal conductivity respectively.

For a forward heat conduction problem, temperature $T$ can be calculated for all points $\boldsymbol{x}$ and time $t$ by using Eqs. (1)–(6) for a given heat flux $q_0(x,t)$ on $\Gamma_0$ in $[0, t_{max}]$. However, in the context of inverse heat conduction problem the heat flux $q_0(x,t)$ is considered to be unknown and is to be estimated. The unknown heat flux $q_0(x,t)$ on $\Gamma_0$ as shown in Fig. 1, is estimated using temperature measurements at a few locations within the domain at some fixed time intervals.

### 2.2. Inverse problem using Bayesian inference

To illustrate the use of Bayesian inference for solving the inverse heat conduction problem, we here consider a forward problem,

$$\boldsymbol{T} = G(\boldsymbol{Z}). \tag{7}$$

Here, $G$ represents the forward model, i.e., the forward heat conduction equation, $\boldsymbol{T}$ denotes the predicted value of temperature at the locations where the temperature is measured. Here, $\boldsymbol{Z} = [q(t_1), q(t_2), \ldots .., q(t_n)]$ which represents an $n$-dimensional vector of discretized heat flux values prescribed at fixed time intervals; we assume a spatially uniform but time-varying heat flux. Here, $\boldsymbol{Z}$ is considered to be the heat flux, although $\boldsymbol{Z}$ could also contain other model parameters such as heat capacity, thermal conductivity or other thermophysical properties. In the Bayesian framework, the unknown heat flux $\boldsymbol{Z}$ is considered to be a time-dependent and/or space-dependent function, and Bayes' rule is used to define a posterior probability density for $\boldsymbol{Z}$, given observed temperature $\boldsymbol{T}_{obs}$. The unknown heat flux is assumed to have a prior probability density of $\pi(\boldsymbol{Z})$ before observing the temperature data $\boldsymbol{T}_{obs}$. Bayesian inference entails prediction of posterior probability density of heat flux $\pi(\boldsymbol{Z}|\boldsymbol{T}_{obs})$ taking into account the observed temperature $\boldsymbol{T}_{obs}$. The observed temperature $\boldsymbol{T}_{obs}$ differs from the predicted temperature $\boldsymbol{T}$ due to measurement uncertainties. The measurement uncertainties are assumed to be additive,

$$\boldsymbol{T_{obs}} = \boldsymbol{T} + \boldsymbol{e} = G(\boldsymbol{Z}) + \boldsymbol{e}, \tag{8}$$

where $\boldsymbol{e}$ denotes measurement errors that are assumed to be independent and identically distributed. Therefore, the probability density of observed temperature given the heat flux is $\pi(\boldsymbol{T}_{obs}|\boldsymbol{Z}) = \pi_e(\boldsymbol{T}_{obs} - G(\boldsymbol{Z}))$, where $\pi_e$ is the probability density of measurement error; $\pi(\boldsymbol{T}_{obs}|\boldsymbol{Z})$ is

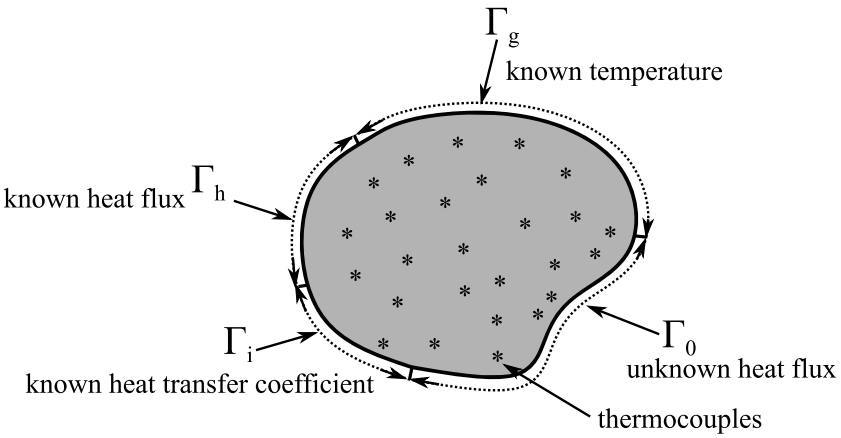


**Fig. 1.** Schematic of the inverse heat conduction problem. The objective is to estimate the unknown boundary heat flux $q_0$ using the temperature measurements $T$ at the thermocouple locations. The boundary conditions on the remaining domain are known.

called the likelihood function. The measurement errors for different observations can be assumed to be independent and hence the likelihood function can be taken as

$$\pi(\boldsymbol{T}_{obs}|\boldsymbol{Z}) = \prod_i \varphi_i(T_{obs,i} - T_i). \tag{9}$$

Here, $\varphi_i$ denotes the probability density of $i$th component of $\boldsymbol{e}$, and $T_i$ and $T_{obs,i}$ are respectively the $i$th component of predicted temperature $\boldsymbol{T}$ and observed temperature $\boldsymbol{T}_{obs}$. Usually, the measurement errors are Gaussian and independently distributed; therefore likelihood function can be simplified to

$$\pi(\boldsymbol{T}_{obs}|\boldsymbol{Z}) \propto \prod_i \exp\left(-\frac{1}{2}\sum \frac{(T_{obs,i} - T_i)^2}{\sigma^2}\right). \tag{10}$$

Here, $\sigma$ is the standard deviation of the measurement noise. The inverse heat conduction problem deals with the calculation of the posterior probability density of the values of the vector $\boldsymbol{Z}$ representing the unknown heat flux given the observed temperature data. To this end, we employ the Bayes' rule

$$\pi(\boldsymbol{Z}|\boldsymbol{T}_{obs}) = \frac{\pi(\boldsymbol{T}_{obs}|\boldsymbol{Z})\pi(\boldsymbol{Z})}{\int \pi(\boldsymbol{Z}|\boldsymbol{T}_{obs})\pi(\boldsymbol{Z})d\boldsymbol{Z}}, \tag{11}$$

$\pi(\boldsymbol{Z}|\boldsymbol{T}_{obs})$ and $\pi(\boldsymbol{Z})$ are called posterior probability density function and prior probability density function, respectively. The vector $\boldsymbol{Z}$ representing the unknown heat flux in the IHCP can be treated as a random process and Bayesian estimation can be used to compute its posterior probability density function. Once $\pi(\boldsymbol{Z}|\boldsymbol{T}_{obs})$ is obtained, the posterior mean estimates of $\boldsymbol{Z}$ can be computed along with their probability bounds.

The prior distribution modeling is required for the representation of the unknown heat flux. We will focus on Bayesian techniques, which use prior information to give a natural mechanism for regularization. Previous studies have used discrete values of $\boldsymbol{Z}$ as unknown parameters to represent the prior. However, one needs to construct a continuous function. Wang and Zabaras [23] have used Markov random field (MRF) for prior modeling of flux. However, MRF requires a larger number of discrete points to represent the field. Therefore, in the current work we represent the random field using K-L expansion which represents it with lesser number of parameters, which are the modes of the K-L expansion. The choice of prior is described below.

### 2.3. Karhunen–Loeve expansion

Typically, in BI-based solution of IHCP, $\boldsymbol{Z}$ is taken as heat flux values at discrete time steps and locations. In most of the previous works, the corresponding prior $\boldsymbol{Z}$ is chosen as a random field to recover the continuous function from finite data. However, the random field requires a large number of discrete points to represent the heat flux. Therefore, in the current work, K-L expansion is considered as an appropriate choice for prior distribution modeling as it represents the heat flux with lesser number of parameters. KL expansion has been successfully used for prior distribution modeling in numerous applications [30,31]. The K-L expansion considers how much data is really needed to capture variation among realizations of unknown random processes [30]. The representation of the heat flux in the form of K-L expansion transforms the inverse problem to inference on a truncated sequence of weights of the K-L modes. K-L expansion not only reduces the dimension of the problem but also cures the ill-posedness of the inverse solution by introducing a regularization term through the prior distribution function.

In the K-L representation, the unknown heat flux $\boldsymbol{Z}$ is parametrized using Karhunen–Loeve expansion and written as,

$$\boldsymbol{Z}(t) = \langle \boldsymbol{Z}(t) \rangle + \sum_{k=1}^{\infty} \sqrt{\lambda_k}\phi_k(t)c_k, \tag{12}$$

where $\lambda_k$ and $\phi_k$ are the ordered eigenvalues and corresponding eigenfunctions of the covariance kernel and $c_k$ are independent standard normal random variables, $c_k \sim \mathcal{N}(0,1)$. In practice, the expansion is truncated at $n$ terms, to obtain an approximate Gaussian random field. The covariance kernel is chosen from the exponential conjugate family given as,

$$C_\theta(t_1,t_2) = \theta \exp\left(-\frac{|t_1 - t_2|^2}{2\tau^2}\right), \tag{13}$$

The correlation time $\tau$ is considered known and the scale $\theta$ of the prior covariance is considered to be a hyperparameter provided with a conjugate inverse gamma hyperprior, $\theta \sim IG(\alpha,\beta)$.

$$p(\theta) = \frac{\beta^\alpha}{\Gamma(\alpha)}\theta^{-\alpha-1}\exp\left(-\frac{\beta}{\theta}\right). \tag{14}$$

The shape parameter $\alpha$ and the scale parameter $\beta$ are taken to be 1. The eigenvalues and eigenfunctions are solved using the Fredholm equation [32],

$$\int_D C(t_1,t_2)\phi_k(t_2)dt_2 = \lambda_k\phi_k(t_1). \tag{15}$$

The covariance kernel $C(t_1,t_2)$ is symmetric and positive definite and using Mercer's theorem [33] can be written as,

$$C(t_1,t_2) = \sum_{k=1}^{\infty} \lambda_k\phi_k(t_1)\phi_k(t_2). \tag{16}$$

Approximating the heat flux by a truncated $n$ term K-L expansion,

$$\boldsymbol{Z}_n(t) = \langle \boldsymbol{Z}(t) \rangle + \sum_{k=1}^{n} \sqrt{\lambda_k}\phi_k(t)c_k. \tag{17}$$

The covariance kernel of $\boldsymbol{Z}_n$ is

$$C(t_1, t_2) = \sum_{k=1}^{n} \lambda_k \phi_k(t_1)\phi_k(t_2), \tag{18}$$

which converges to Eq. (16) as $n \to \infty$ The representation of heat flux using K-L expansion transforms the problem to the prediction of the unknown K-L modes $c_1, c_2, \ldots, c_n$. Therefore, we explore the posterior distribution of the weights $c_k$ of the K-L expansion. Now, we write the posterior density in the form of $c_k$ as,

$$\pi(\boldsymbol{c}, \theta|\boldsymbol{T}_{obs}) \propto \pi(\boldsymbol{T}_{obs}|\boldsymbol{c}) \times \pi(\boldsymbol{c}|\theta) \times \pi(\theta) \propto \prod_i \varphi_i(\boldsymbol{T}_{obs,i} - (\boldsymbol{G}(\boldsymbol{Z}(\boldsymbol{c})))) \times$$

$$\theta^{-n/2}\exp\left(-\frac{\boldsymbol{c}^T\boldsymbol{c}}{2\theta}\right) \times \frac{\beta^\alpha}{\Gamma(\alpha)}\theta^{-\alpha-1}\exp(-\frac{\beta}{\theta}). \tag{19}$$

The MCMC simulations are performed on the posterior distribution of $c_k$. Random walk Metropolis algorithm is used to sample $c_k$ and Gibbs updates are used for the hyperparameter $\theta$. The mean value of $c_k$ is obtained by taking the mean of the posterior distribution of $c_k$ after the burn-in period. Finally, the posterior mean heat flux is computed by using posterior mean values of $c_k$ in Eq. (17). Here, $\theta$ is analogous to the regularization parameter in Tikhonov regularization. Therefore, representing the prior using K-L expansion effectively evaluates the regularization's strength when conditioning on the data. Because of this, regularization in BI leads to the uniqueness of the inverse solution.

### 2.4. Markov chain Monte Carlo (MCMC)

Sampling of the posterior distribution of the K-L modes $c_k$ requires numerical sampling methods because the posterior state space is high dimensional with unknown probability density function. We use the Metropolis–Hastings algorithm [34] to sample the posterior probability density function and the scale parameter $\theta$ is sampled directly from the inverse gamma distribution [30]. The Metropolis–Hastings algorithm is a MCMC method based on the principle that the sampling is done from a Markov chain in such a way that the sampled distribution converges to the target distribution at equilibrium state. In the MCMC method, the sampling is initiated with an initial value of $\boldsymbol{c}^{(\mathbf{0})}$. Then, the next value $\boldsymbol{c}^{(*)}$ is sampled using a proper proposal distribution, which is a conditional distribution on the current state. Thereafter, the ratio of the probability of the new proposed sample ($\pi(\boldsymbol{c}^*)$) to the probability of the current state ($\pi(\boldsymbol{c}^{t-1})$) is calculated as

$$\alpha^* = \frac{\pi(\boldsymbol{c}^*)}{\pi(\boldsymbol{c}^{t-1})}. \tag{20}$$

If the new sample proposed is more likely than the existing sample ($\alpha^* > 1$), the sample is accepted, else the sample is accepted with probability $\alpha^*$. This procedure is repeated until a stationary state is achieved, and the Markov chain approaches the target distribution after a sufficient burn-in period.

### 2.5. The PCE-based surrogate model for fast Bayesian inference

The MCMC method discussed in Section 2.4 can be used to perform BI. However, it involves millions of computations of the forward model for evaluation of the likelihood or posterior at many values of the flux (Eq. (10)), which makes this method computationally expensive. In the current work, we use PCE-based surrogate model to significantly reduce the cost of sampling the posterior density. PCE represents the model predictions in the form of an expansion function of the uncertain model parameters with prior probability distribution functions. The model predictions can be expressed by a series of orthogonal polynomials with respect to the distributions of the uncertain model parameters. We first obtain the PCE-based surrogate model for the exact forward problem, for a prior distribution of heat flux $\boldsymbol{Z}$ represented using K-L modes $c_k$. Thereafter, the PCE surrogate model is used in the MCMC method in Eq. (19), instead of solving the exact forward problem while sampling from the posterior distribution. The use of the PCE surrogate enables computationally efficient sampling from the posterior distribution. We now explain the mathematical formulation of the PCE-based surrogate model.

#### 2.5.1. Mathematical formulation of the PCE surrogate

In terms of the heat flux, we employ a non-intrusive strategy to generate a PCE surrogate for our model predictions, which in this case is the temperature. A detailed discussion on developing a PCE-based surrogate model has been provided by Reagan et al. [35] and we briefly summarize the procedure here. In the PCE method, we propagate the variability in model parameters to model predictions by introducing additional stochastic dimensions $\boldsymbol{\xi} = [\xi_1, \xi_2, \xi_3, \ldots \xi_n]$, corresponding to $n$ uncertain model parameters. Because, we represent the heat flux using the K-L expansion, the model parameters are the K-L modes $c_k$. The stochastic dimensions $\xi_k \sim \mathcal{N}(0, 1)$ are selected as a random variable with standard normal probability density function for normally distributed model parameters. Therefore, the normally distributed K-L modes can be written in terms of the random variable $\xi_k$ as

$$c_k = \mu_k + \sigma_k\xi_k, \tag{21}$$

where $\mu_k$ and $\sigma_k$ are the mean and standard deviation of the prior distribution of the K-L mode $c_k$. The model prediction such as temperature, denoted by $T$ is expressed using PCEs [36] as

$$T(\boldsymbol{x}, t, \boldsymbol{\xi}) = \sum_{k=0}^{\infty} T_k(\boldsymbol{x}, t)\boldsymbol{\Psi}_k(\boldsymbol{\xi}), \tag{22}$$

where, $T_k$ represents the coefficients of the temperature at that location and time and $\boldsymbol{\Psi}_k$ are the basis functions of the PCE. The choice of the basis functions depends on the distribution of random variables ($\boldsymbol{\xi}$). The basis functions are orthogonal to each other, with the probability density as the weighing function. In the present case, the random variables are assumed to follow normal distribution. Therefore, the polynomial basis chosen are Hermite polynomials [35].

For one uncertain normally distributed parameter, the basis functions $\boldsymbol{\Psi}_k = \psi_k$ are one-dimensional Hermite polynomials.

$$\psi_0 = 1, \psi_1 = \xi, \psi_2 = \xi^2 - 1, \psi_3 = \xi^3 - 3\xi. \tag{23}$$

For practical purpose, the infinite series in Eq. (22) is truncated to a fixed order $P$, which is the order of the highest polynomial required to construct the PCE. Therefore, for the case of one uncertain parameter, the total number of terms in PCE is $P + 1$. In general, for $n$ dimensions and highest order of polynomial as $p$, the total number of terms in PCE in Eq. (22) is $P + 1$ given as

$$P + 1 = \frac{(p + n)!}{p!n!}. \tag{24}$$

The PCE basis functions $\boldsymbol{\Psi}_k(\boldsymbol{\xi})$ are $n$-dimensional Hermite polynomials which are the product of one dimensional Hermite polynomials. The Hermite polynomials involve multi-index $m_k^i$.

$$\boldsymbol{\Psi}_k(\boldsymbol{\xi}) = \prod_{i=1}^{n} \psi_{m_k^i}(\xi_i). \tag{25}$$

The first few 2-D Hermite polynomials for two uncertain model parameters ($n = 2$), are given by

$$\begin{aligned}
\boldsymbol{\Psi}_0(\boldsymbol{\xi}) &= \psi_0(\xi_1)\psi_0(\xi_2) = 1,\\
\boldsymbol{\Psi}_1(\boldsymbol{\xi}) &= \psi_1(\xi_1)\psi_0(\xi_2) = \xi_1,\\
\boldsymbol{\Psi}_2(\boldsymbol{\xi}) &= \psi_0(\xi_1)\psi_1(\xi_2) = \xi_2,\\
\boldsymbol{\Psi}_3(\boldsymbol{\xi}) &= \psi_2(\xi_1)\psi_0(\xi_2) = \xi_1^2 - 1,\\
\boldsymbol{\Psi}_4(\boldsymbol{\xi}) &= \psi_1(\xi_1)\psi_1(\xi_2) = \xi_1\xi_2,\\
\boldsymbol{\Psi}_5(\boldsymbol{\xi}) &= \psi_0(\xi_1)\psi_2(\xi_2) = \xi_2^2 - 1.
\end{aligned} \tag{26}$$

We compute the coefficients $T_k$ of the corresponding PCE of temperature in Eq. (22) to describe the dependence of temperature on

the uncertain model parameters. To this end, we truncate Eq. (22) to $P$ terms and estimate the coefficients $T_k$ using the orthogonality of Hermite polynomials with respect to the standard normal probability density function $f(\xi)$ and project the PC expansions onto the PC basis to get

$$T_k(\boldsymbol{x},t) = \frac{\int_{-\infty}^{\infty} T(\boldsymbol{x},\xi,t)\Psi_k(\xi)f(\xi)d\xi}{\int_{-\infty}^{\infty}\Psi_k^2(\xi)f(\xi)d\xi} = \frac{\langle T\Psi_k\rangle}{\langle\Psi_k^2\rangle}. \tag{27}$$

The integrals in the numerator and denominator of Eq. (27) can be approximated using weighted average of functional values at specific points within the domain of integration which can be evaluated by numerical Gauss–Hermite quadrature. For a single uncertain parameter ($n = 1$), the coefficients $T_k(\boldsymbol{x},t)$ of the PC expansion can be calculated as

$$T_k(\boldsymbol{x},t) = \frac{\sum_{j=1}^{N} T(\boldsymbol{x},t,\xi^{(j)})\Psi_k(\xi^{(j)})w^{(j)}}{\sum_{j=1}^{N}\Psi_k^2(\xi^{(j)})w^{(j)}}. \tag{28}$$

Here, $w^{(j)}$ is the weight corresponding to the quadrature point and $N$ is the total number of quadrature points required to accurately approximate the integral. The terms $T(\boldsymbol{x},t,\xi^{(j)})$ are computed using the forward model using the model parameters corresponding to $\xi^{(j)}$.

In general, for $n$ number of uncertain parameters, the quadrature points at which deterministic calculations are performed are given by the $n$-dimensional tensor product of one-dimensional quadrature points. Therefore, as the number of uncertain parameters increases, the number of solutions of the forward model required to perform numerical integration increases exponentially as $N^n$. To overcome this limitation, in the current work, we use Smolyak quadrature [37] which requires significantly less number of quadrature points to perform numerical integration with reasonable accuracy. Solving for the coefficients of PCE yields the surrogate model for the forward problem. Thereafter, we use the surrogate model in Eq. (10) to predict the temperature to propagate uncertainty from prior distribution of model parameters to model predictions. The calculation of temperature using the surrogate model instead of solving the full forward model in Eq. (19) accelerates the BI based solution to the inverse problem. In addition, knowing the PCEs, we can also compute the various statistical moments such as mean and standard deviation of temperature. The mean is given by the zeroth-order coefficient $T_0$ because the expectation $\langle\Psi_k\rangle = 0$ for $k > 0$ and the variance is calculated using the higher-order coefficients. The variance of temperature is calculated by,

$$\mathrm{Var}(T) = \langle(T - \langle T\rangle)^2\rangle = \sum_{k=1}^{P} T_k^2\langle\Psi_k^2\rangle. \tag{29}$$

## 3. Results and discussion

In this section, we demonstrate the introduced dimensionality reduction and fast Bayesian inference approach on three inverse heat conduction problems. The problems consist of estimating unknown time-varying heat flux using the proposed approach. The first problem is a classical one-dimensional IHCP in which transient boundary heat flux on a slab is estimated using the temperature measurements at a certain location within the slab. The second problem involves a two-dimensional disc brake system in which heat flux of the disc is estimated using temperature measurements taken within the disc. The third problem consists of a sounding rocket system in which the surface heat flux on the rocket module is estimated using temperature measurements inside the rocket shell.

### 3.1. Heat flux estimation in one-dimensional heat conduction

We begin by considering the IHCP of boundary heat flux estimation for a 1-D slab as shown in Fig. 2. A transient heat flux $q(t)$ is applied at $x = 0$ and the slab is insulated at the other end ($x = L$). Initially, the slab has a uniform temperature ($T = T_0$). The governing equation

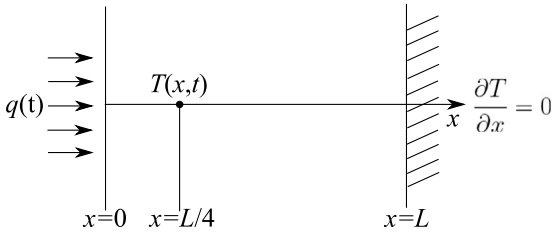


**Fig. 2.** Schematic illustrating the one-dimensional inverse heat conduction problem in a slab. The transient boundary heat flux $q(t)$ is estimated using the temperature measurements at the sensor placed at $x = L/4$.

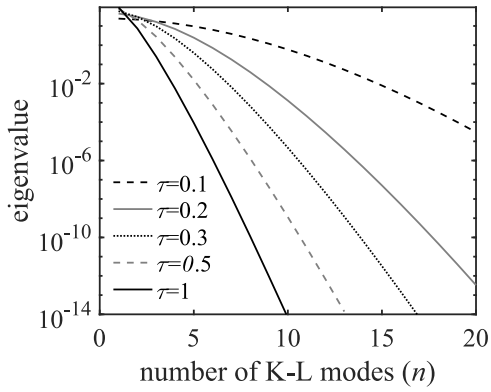


**Fig. 3.** Decay in eigenvalue of the triangular profile for varying K-L modes with different prior correlation times $\tau$.

and the corresponding initial and boundary conditions to solve the one-dimensional forward problem are given as,

$$\frac{\partial T}{\partial t} = \alpha\frac{\partial^2 T}{\partial x^2}, \quad t > 0, \quad 0 < x < L, \tag{30}$$

$$T(x,0) = T_0, \quad 0 \le x \le L, \tag{31}$$

$$\left.\frac{\partial T}{\partial x}\right|_{x=L} = 0, \quad t > 0, \tag{32}$$

$$-k\left.\frac{\partial T}{\partial x}\right|_{x=0} = q(t), \quad t > 0, \tag{33}$$

where, $\alpha = k/\rho c_p$. Now we introduce the following dimensionless variables,

$$\tilde{x} = \frac{x}{L}, \quad \tilde{t} = \frac{\alpha t}{L^2}, \quad \tilde{T} = \frac{T - T_0}{T_{ref} - T_0}, \quad \tilde{q}(\tilde{t}) = \frac{qL}{k(T_{ref} - T_0)}, \tag{34}$$

where, $T_{ref}$ is some arbitrary reference temperature different from the initial temperature. On non-dimensionalizing Eqs. (30)–(33) using the dimensionless expressions in Eq. (34), the non-dimensional equations to solve the one-dimensional forward problem are given as,

$$\frac{\partial\tilde{T}}{\partial\tilde{t}} = \frac{\partial^2\tilde{T}}{\partial\tilde{x}^2}, \quad \tilde{t} > 0, \quad 0 < \tilde{x} < 1, \tag{35}$$

$$\tilde{T}(\tilde{x},0) = 0, \quad 0 \le \tilde{x} \le 1, \tag{36}$$

$$\left.\frac{\partial\tilde{T}}{\partial\tilde{x}}\right|_{\tilde{x}=1} = 0, \quad \tilde{t} > 0, \tag{37}$$

$$-\left.\frac{\partial\tilde{T}}{\partial\tilde{x}}\right|_{\tilde{x}=0} = \tilde{q}(\tilde{t}), \quad \tilde{t} > 0. \tag{38}$$

The forward problem described by Eqs. (35)–(38) involves the estimation of the temperature $\tilde{T}(\tilde{x},\tilde{t})$ in the region $0 < \tilde{x} < 1$ when the flux $\tilde{q}(\tilde{t})$ is known. For convenience, we henceforth remove the

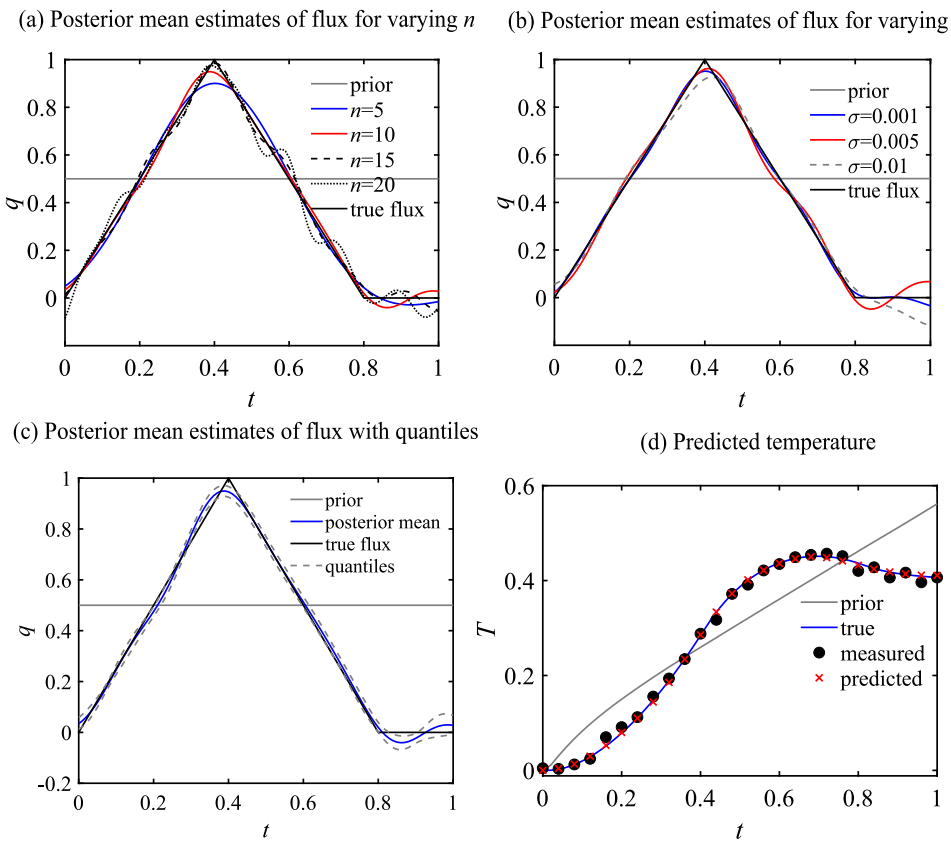


**Fig. 4.** The prediction of the unknown transient heat flux using the PCE-based BI framework. (a) Posterior mean estimate of heat flux for varying number of terms ($n$) in K-L expansion. The posterior transient heat flux matches well with the true heat flux and an optimum solution is obtained at $n = 10$. (b) Posterior mean estimate for varying $\sigma$. (c) Posterior mean estimate and associated 5%–95% quantiles from the MCMC samples. The probability bounds indicate the range in which the predicted flux can lie with the associated uncertainty in the measured temperature. (d) Predicted temperature using the predicted heat flux for $n = 10$, which matches well with the measured data.

symbol ~(tilde) while representing the dimensionless variables in the current section. For a known heat flux $q(t)$, the temperature $T(x,t)$ is obtained by numerically solving the equations using second-order finite difference scheme to calculate the spatial derivatives and Runge–Kutta fourth-order scheme for time integration. The domain was discretized using 201 equispaced grid points. A fixed time step of 0.01 was used for time integration. The chosen grid and time-step ensured a converged solution by comparing the simulation with various analytical solutions. The inverse problem involves the estimation of the time-varying heat flux given temperature measurements at a particular location ($x = L/4$) at fixed time intervals. The inverse problem is solved for four different flux profiles: a triangular flux, a step function, a sine–cosine function of flux, and a triangular-sine function of flux.

We now discuss the results obtained using the triangular heat flux profile. We represented the prior heat flux $q(t)$ using K-L expansion with mean $\langle \boldsymbol{Z}(t) \rangle = 0.5$ and Gaussian covariance kernel $C(t_1, t_2)$ given by Eq. (13). To represent the prior heat flux $q(t)$ using K-L expansion we first determine the eigenfunctions and eigenvalues appearing in the K-L expansions. Fig. 3 shows the decay of K-L eigenvalues with increasing $n$ for triangular heat flux profile with different values of prior correlation time $\tau$. The eigenvalues decay exponentially fast for larger correlation time $\tau$ which shows that large number of K-L modes are required to obtain accurate solutions for functions with shorter prior correlation time. For all our simulations, correlation time of $\tau = 0.1$ is chosen.

We initially obtained the PCE surrogate model for temperature based on the prior probability distribution of the heat flux based on $n = 10$ K-L modes. We choose the nodes of the Smolyak quadrature as discussed in Section 2.5.1 as the priors of $c_k$. We construct the prior heat flux using the priors of $c_k$. We obtained the surrogate model of temperature using second-order PCEs, which consisted of sixty-six coefficients for representing the flux with $n = 10$ K-L modes which was sufficient to obtain the surrogate model. This corresponds to $N = 221$ simulations.

We now solve the inverse problem to estimate the unknown heat flux. To simulate the measured temperature data, we performed a deterministic simulation on a known heat flux which we call as the true value and added noise to it. Simulated measurement temperature data at $x = 0.25$ (considered as the thermocouple location) and at time intervals of 0.05 are generated by adding Gaussian random noise to the obtained temperature $T$. Three different standard deviation values $\sigma = 0.001, 0.005$ and 0.01 are considered to add noise to the corresponding temperature data. This temperature measurement is considered as the measured data to estimate the transient heat flux. We performed the MCMC sampling to obtain the posterior probability distribution of the estimated values of K-L modes. We used the PCE surrogate model to obtain the inverse solution using BI.

Fig. 4(a) shows the posterior mean estimate of the heat flux for varying number of K-L modes $n$ used to represent the heat flux and the true heat flux. Once we obtained the posterior distribution, we calculated the posterior mean by taking an average of all the samples. We observe that $n = 10$ K-L modes are sufficient to obtain the heat flux. Fig. 4(b) shows the posterior mean estimate of the heat flux for the three different standard deviations. The posterior mean estimate is not sensitive to the value of $\sigma$ which suggests that the statistical information of measurement noise is not necessary for the point estimate of the posterior flux. However the probability estimate of the predicted flux, depends on the measurement noise $\sigma$. Fig. 4(c) shows the posterior mean estimate with associated 5% and 95% quantiles of the estimates. The uncertainty in the predicted flux is highest near the boundaries and at the peak flux. Fig. 4(d) shows the temperature predicted by using

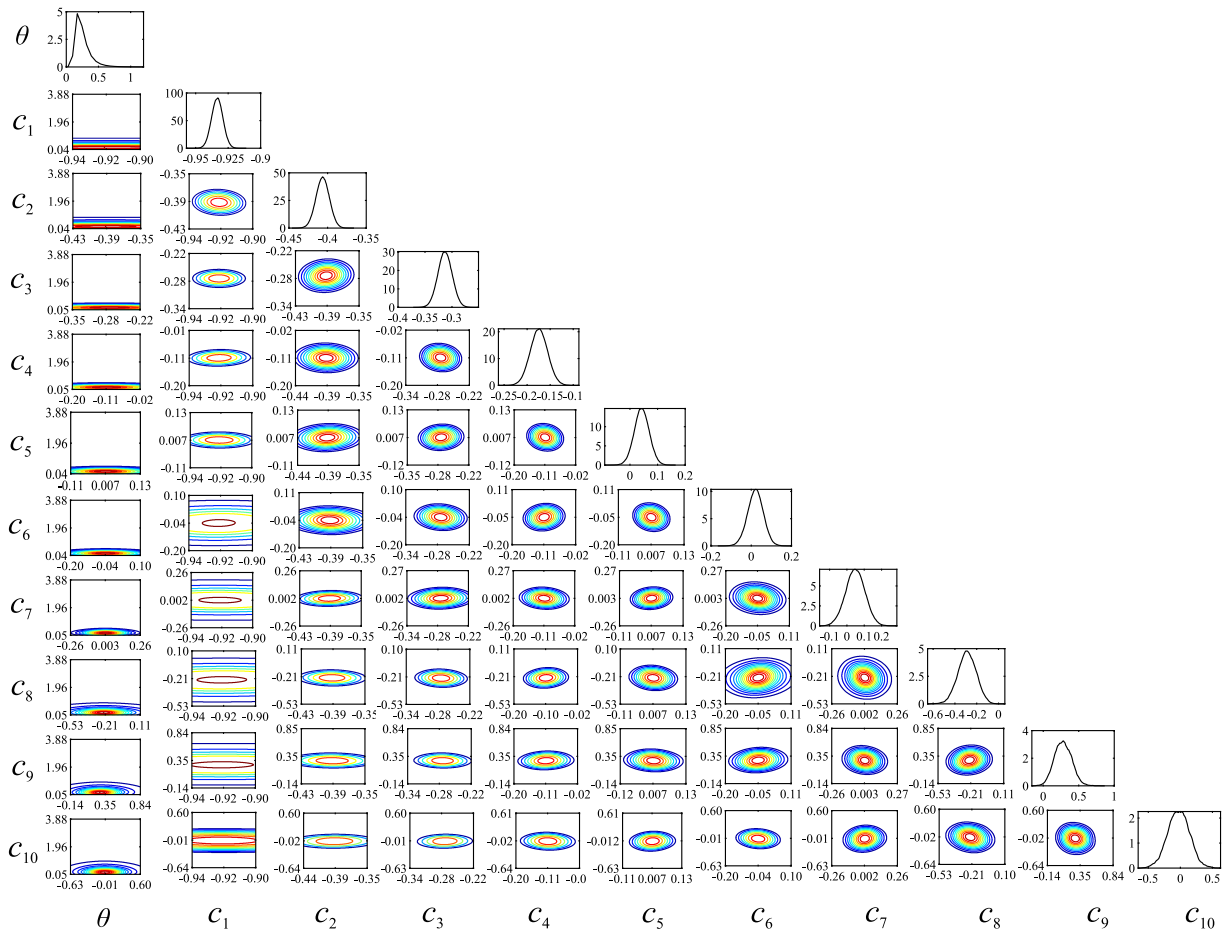


**Fig. 5.** 1-D and 2-D posterior marginals of the K-L mode strengths $c_i$ and the hyperparameter $\theta$ for the triangular heat flux profile with correlation time $\tau = 0.1$ for measurement noise $\sigma = 0.001$.

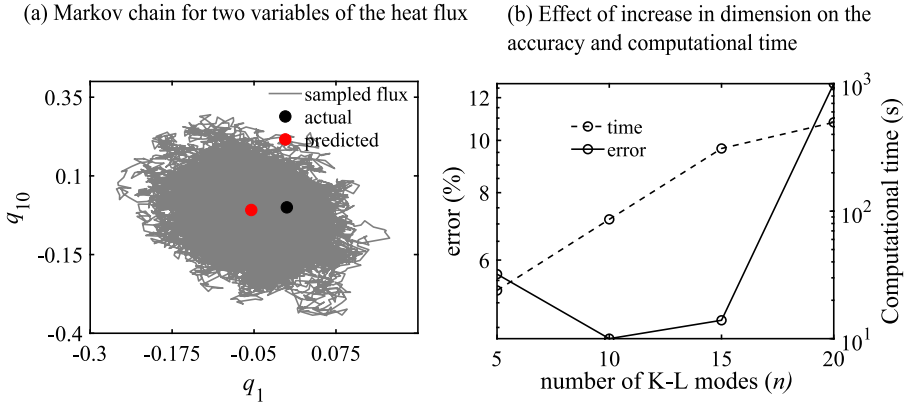


**Fig. 6.** Covergence of the flux values obtained from the K-L modes and the variation in accuracy and computational time with increase in the number of K-L modes of the heat flux. (a) Markov chain convergence of 1 million MCMC samples for two parameters of the flux vector for the triangular heat flux profile. The values converge to the true value. (b) Variation of the accuracy and computational time with an increase in the dimension of the heat flux represented using the K-L modes. The accuracy increases with an increase in dimension until the minimum dimension of the K-L modes to reconstruct the heat flux accurately is obtained. The accuracy falls on further increase in dimension of the K-L modes of the heat flux. As expected, the computational time increases with increase in dimensions.

the posterior mean heat flux at $x = 0.25$. The predicted temperature matches the forward model with the measured data. The match between the measured and predicted temperature shows the applicability of the fast BI framework to solve IHCP.

Fig. 5 shows the one and two-dimensional posterior marginals of the hyperparameter $\theta$ and the modes $c$ obtained for the triangular heat flux profile. Significant correlations are observed between the lower-indexed modes and between the modes and hyperparameter $\theta$. The higher indexed modes seem to be uncorrelated and mutually independent as observed from their 2-D marginals. The marginal distributions of $c_7, c_8, c_9$ and $c_{10}$ are quite similar in shape with mutually weak correlations among them.

We now discuss the convergence, computational time and accuracy of the heat flux obtained using the K-L modes for the triangular heat flux profile. We show the convergence of the Markov chain for two values of the heat flux profile corresponding to first and tenth mode

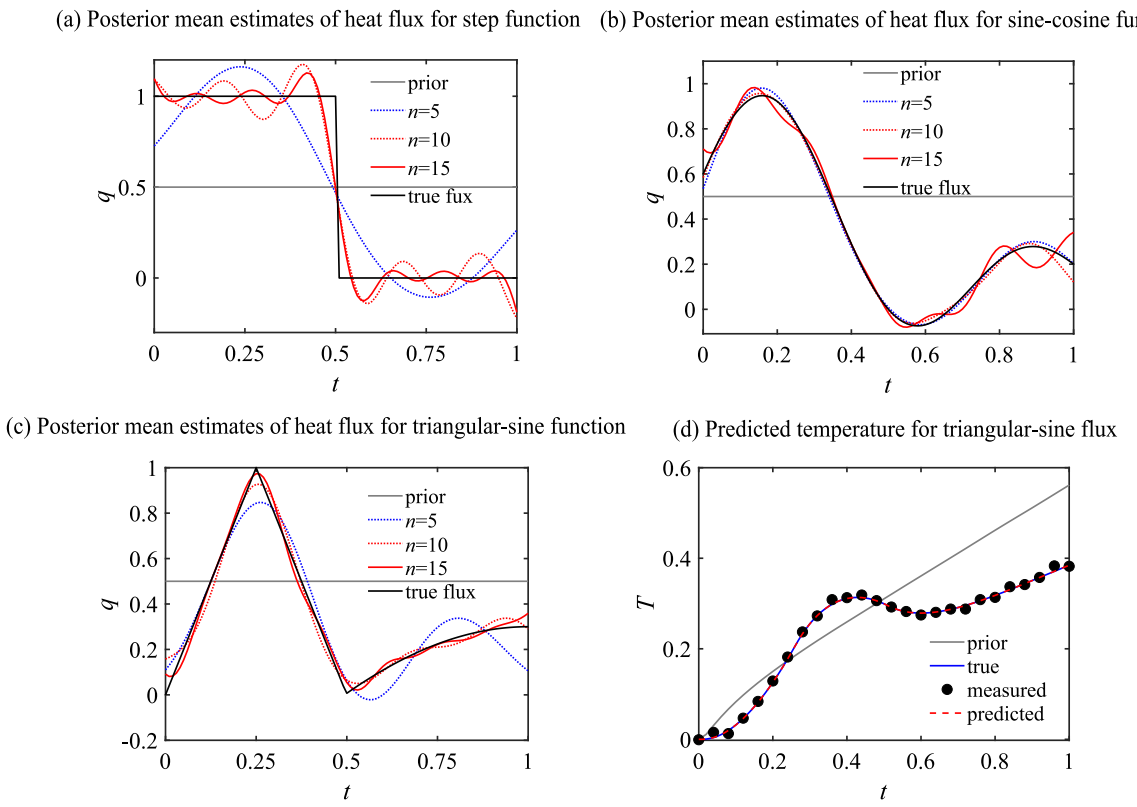


**Fig. 7.** The prediction of the unknown transient heat flux using the PCE-based BI framework for different flux profiles. (a)–(c) Posterior mean estimate of heat flux for varying number of terms ($n$) in K-L expansion for different flux profiles. The posterior transient heat flux matches with the true heat flux and an optimum value is obtained at $n = 15$ for step function of flux, at $n = 5$ for sine–cosine function of flux and at $n = 15$ for triangular-sine function of flux. (d) Predicted temperature using the predicted heat flux for $n = 15$ for triangular-sine function of flux shown in (c).

when it is represented using $n = 10$ K-L modes, in Fig. 6(a). After a given number of samples, convergence is attained, and predicted values closely match true values. Fig. 6(b) shows the effect of dimension $n$ of the K-L modes of the heat flux on the accuracy of the estimated posterior and the computational time. Initially, the accuracy increases with an increase in the dimension since higher dimensions can represent the heat flux accurately. However, once the minimum number of K-L modes required to reconstruct the heat flux is obtained, the accuracy falls on further increase in dimension due to overfitting. Hence, an optimum dimension to reconstruct the heat flux is required. As expected the computational time increases with increase in dimension as shown in Fig. 6(b).

To check the efficiency of the PCE surrogate, the corresponding Monte Carlo simulations were performed where instead of using the PCE surrogate to solve the inverse problem, deterministic simulations were used to solve the forward problem. To compare the two solutions, simulations with one million sample size of the Markov chain were performed using the standard Monte Carlo approach to achieve comparable accuracy. The same accuracy can be achieved using the two methods leading to a speed-up factor of 2000 using the PCE surrogate model.

We now present the results for a few other heat flux profiles such as step profile, sine–cosine profile, and triangular-sine profile of flux. All other parameters were same as the IHCP for triangular heat flux. Figs. 7(a)–(c) show the inverse solution for several heat flux profiles with varying number of K-L modes. Fig. 7(a) shows a step function of heat flux. The approach could recover a challenging case of discontinuous function correctly, albeit with some oscillations. The number of K-L modes required to predict an approximate heat flux is $n = 15$. Fig. 7(b) shows a function given by the equation $q = (1 + \sin(\pi t) + \cos(\pi t) + \sin(2\pi t) + \cos(2\pi t) + \sin(3\pi t))/5$. Only $n = 5$ K-L modes are required to predict the heat flux profile. Fig. 7(c) shows a triangular-sine function

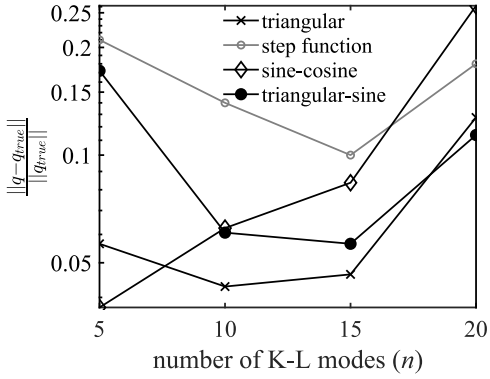


**Fig. 8.** The ratio of the norm of differences in posterior mean estimate of heat flux and the respective true heat flux values to the norm of true heat flux for different heat flux profiles with varying K-L modes.

of heat flux profile. For the triangular-sine function of heat flux, $n = 15$ K-L modes are required to predict the profile accurately. The difference in the number of modes required to predict the profile accurately for each flux reflects the fact that the number of K-L modes required for any profile is dependent on the smoothness of the actual flux function being estimated. Fig. 7(d) shows the predicted temperature obtained using the posterior mean heat flux for the triangular-sine profile. The predicted temperature matches well with the measured data.

Fig. 8 shows the ratio of the norm of the difference in posterior mean estimate of heat flux and the true value of heat flux to the norm of true heat flux for different heat flux profiles for varying number of K-L modes. The figure shows the minimum number of K-L modes required to obtain an accurate flux profile. For the sinusoidal cosine profile of

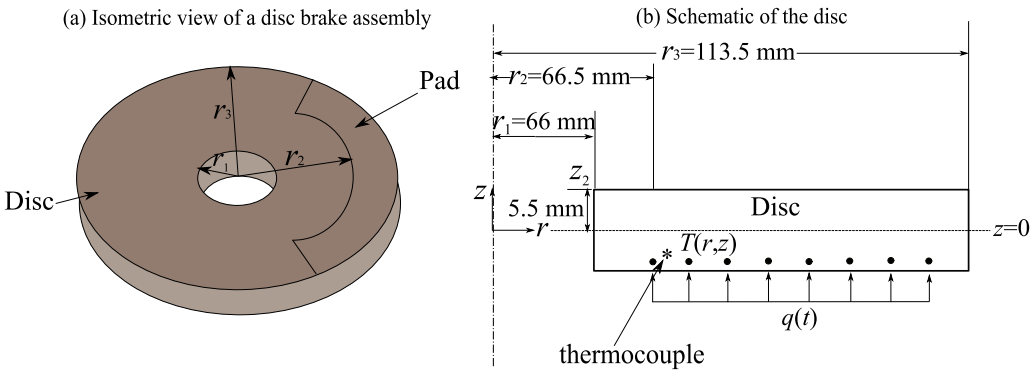


**Fig. 9.** Schematic of the disc brake assembly. (a) A disc brake system to show the disc and the pad. The inverse heat conduction problem involve estimating the heat generated into the disc during the course of braking. (b) Schematic of the disc. The disc pad configuration is symmetrical to the center line so only half of the disc is considered as the computational domain. $q(t)$ is the boundary heat flux which is the heat dissipated into the disc. $r_1$ and $r_3$ are the inner and outer disc diameter. $r_3 - r_2$ is the sliding radius of the disc.

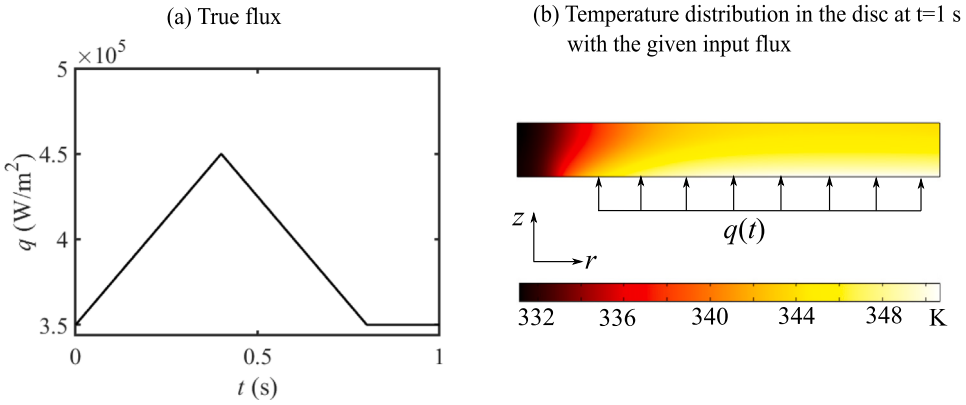


**Fig. 10.** Temperature distribution in the disc at $t = 1$ s for the given input heat flux. (a) shows the transient input heat flux into the disc. (b) is the temperature distribution obtained in the computational domain at $t = 1$ s.

flux, the minimum number of modes required is 5, whereas 10 modes are required for triangular profile and 15 modes are required for step function and triangular-sine profile of heat flux. The minimum number of K-L modes required to obtain an approximate solution of the heat flux profile depends on the smoothness of the heat flux function. The smooth heat flux profiles yield a minimum at smaller number of K-L modes than the non-smooth heat flux profiles.

### 3.2. Heat flux estimation in 2D heat conduction

In this model problem, we estimate the time-dependent heat flux in a disc brake system using temperature measurements at a particular location in the disc. Fig. 9(a) shows an isometric view of a disc brake system, while the schematic of the heat transfer problem of the disc is shown in Fig. 9(b). During the braking process, frictional heat is generated at the disc pad interface which is then dissipated into the disc and pad. The dissipated heat is considered as the boundary heat flux into the disc and is to be estimated. We model the transient heat conduction in the disc using the following governing equations and boundary and initial conditions.

$$\frac{1}{r}\frac{\partial}{\partial r}\left[kr\frac{\partial T(r,z,t)}{\partial r}\right]+\frac{\partial}{\partial z}\left[k\frac{\partial T(r,z,t)}{\partial z}\right]=\rho c_p\frac{\partial T(r,z,t)}{\partial t} \quad \text{in} \quad r_1<r<r_3,\ 0<z<z_2,\quad t>0, \tag{39}$$

$$-k\frac{\partial T(r,z,t)}{\partial r}=h[T_\infty - T(r,z,t)], \quad \text{at} \quad r=r_1,\quad 0<z<z_2,\quad t>0, \tag{40}$$

$$k\frac{\partial T(r,z,t)}{\partial r}=h[T_\infty - T(r,z,t)], \quad \text{at} \quad r=r_3,\quad 0<z<z_2,\quad t>0, \tag{41}$$

$$k\frac{\partial T(r,z,t)}{\partial z}=0, \quad \text{at} \quad z=0,\quad r_1<r<r_3,\quad t>0, \tag{42}$$

$$k\frac{\partial T(r,z,t)}{\partial z}=h[T_\infty - T(r,z,t)], \quad \text{at} \quad z=z_2,\quad r_1<r<r_2,\quad t>0, \tag{43}$$

$$k\frac{\partial T(r,z,t)}{\partial z}=q(t), \quad \text{at} \quad z=z_2,\quad r_2<r<r_3,\quad t>0, \tag{44}$$

$$T(r,z,0)=T_0, \quad \text{for} \quad r_1<r<r_3,\quad 0<z<z_2,\quad t=0. \tag{45}$$

In Eq. (44), $q(t)$ is the frictional heat flux into the disc. Here, we have assumed a uniform wear contact, and hence the heat flux is only a function of time and independent of $r$. Also, since the disc brake system is symmetrical to the centerline $z = 0$, we consider only half of the disc as the computational domain. The temperature gradient in the tangential direction is neglected due to the very fast rotation of the disc during the braking process. The values of $k$, $\rho$, $c$ and $h$ were taken as 76.2 W m$^{-1}$ K$^{-1}$, 7870 kg m$^{-3}$, 440 J kg$^{-1}$ K$^{-1}$, and 60 W m$^{-2}$ K$^{-1}$ respectively. The ambient temperature was taken as $T_\infty = 293.15$ K, and the initial temperature of the disc was considered as $T_0 = 313.15$ K.

The temperature distribution of direct solution using the triangular function of heat flux is shown in Fig. 10. The numerical procedure used in this problem is based on the finite-element method with linear shape functions on structured mesh and backward difference formula (BDF) based time integration. The grid-independence test and time-step-interval independent solutions were performed on the model using the implicit time stepping scheme. To solve the inverse problem, the

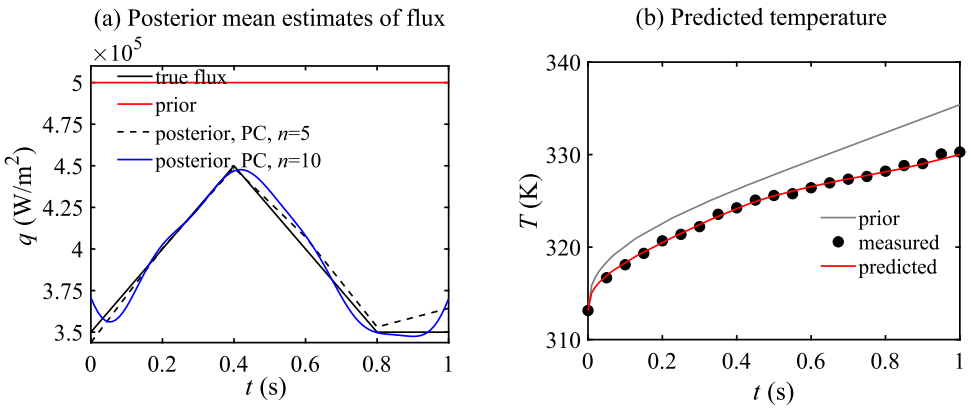


**Fig. 11.** Prediction of the unknown transient heat flux using the PCE-based BI framework for the disc brake system. (a) The posterior mean estimate of heat flux by assuming the prior heat flux with $n = 5$ and $n = 10$ K-L modes. (b) Predicted temperature obtained using the predicted heat flux for $n = 10$ K-L modes, which matches well with the measured data.

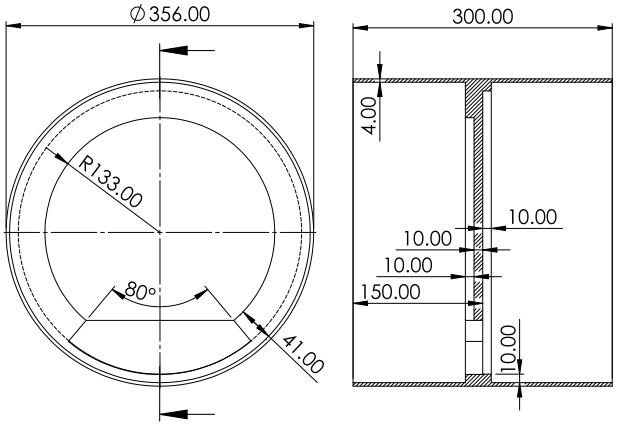


**Fig. 12.** Geometry of the rocket module. The configuration is symmetrical to the center line so only half of the geometry is considered as the computational domain. The dimensions are in mm.

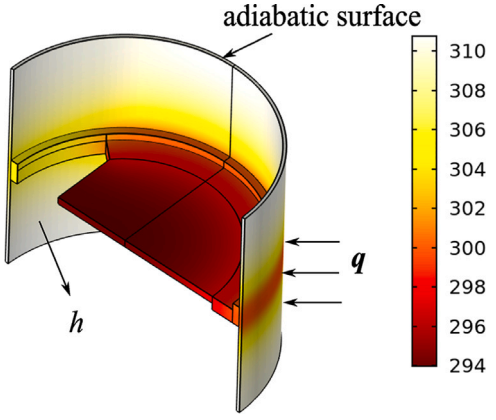


**Fig. 13.** Physical model of rocket module showing the boundary conditions and the temperature distribution for a constant heat flux $q = 2000$ W m$^{-2}$ and at $t = 400$ s.

heat flux into the disc during a braking process is considered unknown and is estimated. To get the measured temperature data to solve the inverse problem, we performed a deterministic simulation on a prior known function of heat flux which we call true value. We used the temperature at $r_0 = 68$ mm, $z_0 = 2.2$ mm and added Gaussian random noise with $\sigma = 0.2$ to mimic measurement errors. Using the temperature measurements, we predict the unknown K-L modes $c_k$ of the flux profile using the fast BI framework. The correlation time $\tau = 0.1$ was used for all the simulations. A uniform prior of $q = 5 \times 10^5$ W m$^{-1}$ was used to obtain the surrogate model. We obtained the surrogate model of temperature using second-order PCEs, which consisted of sixty-six coefficients for representing the heat flux with $n = 10$ K-L modes which was sufficient to obtain the surrogate model. This corresponds to $N = 221$ deterministic simulations of the disc brake system. These 221 deterministic simulations required 20 min. The posterior distributions of the modes are estimated with long Markov chains of one million samples which are enough for sampling from the converged posterior. These one million samples were obtained in 55 s using the surrogate PC model which is very much computationally efficient in comparison to the forward runs. All simulations were performed on Intel i5 3.2 GHz, 12 GB RAM personal computer.

Fig. 11(a) shows the prior mean estimate of heat flux and the true heat flux. Fig. 11(a) also shows the posterior mean estimate obtained using the PCE surrogate by discretizing the prior heat flux using $n = 5$ and $n = 10$ K-L modes. The posterior mean estimate of heat flux obtained using the PCE surrogate is in good agreement with the true heat flux profile. The results show that heat flux can be accurately predicted using the proposed framework for realistic problems. Fig. 11(b) shows the predicted temperature obtained using the posterior mean heat flux. The match between the measured and predicted temperatures shows the efficacy of the fast BI framework to solve IHCPs.

## 4. Heat flux estimation in three-dimensional sounding rocket module

In this model problem, we solve an inverse heat conduction problem to estimate the transient heat flux on the surface of a three-dimensional sounding rocket module using the recorded temperature profile inside the rocket shell. The rocket body is made up of aluminium which consists of a thick bulkhead with a hole attached to a cylindrical rocket. This bulkhead is centered around a REXUS sounding rocket. The geometry has been adopted from Dabrowski et al. [38] and is depicted in Fig. 12. We model the transient heat conduction in the rocket module using the three-dimensional heat conduction equation given by Eq. (1).

The values of $k$, $\rho$ and $c_p$ are 130 W m$^{-1}$ K$^{-1}$, 960 J kg$^{-1}$ K$^{-1}$, and 2810 kg m$^{-3}$, respectively. A heat flux $\boldsymbol{q}$ is present at the outer surface as shown in Fig. 13. The inner surface is exposed to convection with a convective heat transfer coefficient $h = 5$ W m$^{-2}$ K$^{-1}$. Since it is anticipated that other rocket modules comparable to the one being described are positioned above and below it, we used adiabatic boundary conditions on the top and bottom surfaces as shown in Fig. 13. The ambient temperature was taken as $T_\infty = 283.15$ K and the initial temperature of the rocket surface was considered as $T_0 =$

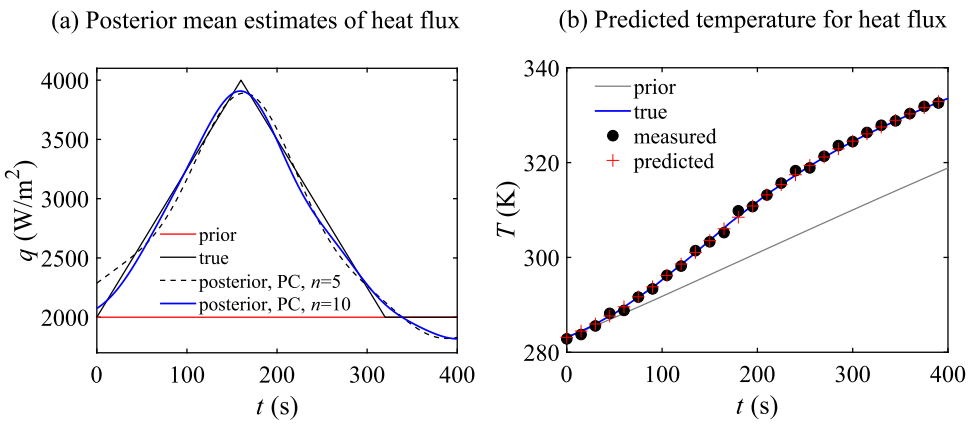


**Fig. 14.** Prediction of the unknown transient heat flux using the PCE-based BI framework for the rocket module. (a) The posterior mean estimate of heat flux by assuming the prior heat flux with $n = 5$ and $n = 10$ K-L modes. (b) Predicted temperature obtained using the predicted heat flux for $n = 10$ K-L modes, which matches well with the measured data.

283.15 K. The finite-element method on unstructured mesh and backward difference formula-based time integration are used to solve this problem numerically. With the implicit time-stepping scheme, the grid independence and time-step interval independent tests were done on the model. COMSOL Multiphysics 5.5 was used to do the calculations, and the material properties were based on the properties of Al7075. The simulation was performed for 400 s, and simulation data was saved at a time interval of 1 s. To illustrate the forward problem in Fig. 13, we show the temperature prediction for a case with a constant heat flux $q = 2000$ W m$^{-2}$ and at $t = 400$ s.

To solve the inverse problem, the heat flux on the outer surface of the module is considered unknown and is estimated. To get the measured temperature data to solve the inverse problem, we performed a deterministic simulation using a triangular-shaped heat flux function which we call as the true value as shown in Fig. 14(a). We used the temperature at time intervals of 10 s at $x = 124$, $y = 20$ and $z = 121$ mm. The noisy measured data with $\sigma = 0.5$ to mimic measurement errors is also shown in Fig. 14(a). Using the temperature measurements, we predicted the unknown K-L modes $c_k$ of the flux profile using the fast BI framework described in Section 2. The correlation time $\tau = 40$ s was used for all the simulations. A uniform prior of $q = 2000$ W m$^{-2}$ was used to obtain the surrogate model. We obtained the surrogate model of temperature using second-order PCEs, which consisted of sixty-six coefficients for representing the heat flux with $n = 10$ K-L modes. This corresponds to $N = 21$ deterministic simulations of the rocket module. The accuracy of the surrogate model was checked by taking more number of deterministic simulations than $N = 21$. The 21 deterministic forward simulations, which required total 24 min of computational time, were sufficient to obtain an accurate PCE surrogate.

Fig. 14(a) also shows the posterior mean estimate obtained for the triangular heat flux profile using the PCE surrogate by discretizing the prior heat flux using $n = 5$ and $n = 10$ K-L modes. The posterior mean estimate of heat flux obtained using the PCE surrogate is in good agreement with the true heat flux profile. The results show that heat flux can be accurately predicted using the proposed framework for realistic problems. The prediction of the posterior distributions of the K-L modes of the heat flux using BI typically requires long Markov chains with millions of samples since they allow for accurate sampling from the converged posterior. Using a surrogate PC model, which is far more computationally efficient than forward runs, these one million samples were collected in 2.4 min which would have required many days to run using the full forward model. Fig. 14(b) shows the predicted temperature obtained using the posterior mean heat flux. The match between the measured and predicted temperatures for the three-dimensional problem shows the efficacy of the fast BI framework to solve IHCPs irrespective of the size and geometry of the problem.

## 5. Conclusion

We have demonstrated a computationally-efficient Bayesian approach to inverse problems to determine the unknown time-dependent heat flux into inverse heat conduction problems, knowing the temperature history at certain measurement locations. A dimensionality reduction technique is introduced in which the unknown heat flux is represented in the form of Karhunen–Loeve expansion to parametrize it with fewer degrees of freedom. The use of polynomial chaos expansions as a surrogate model for efficient uncertainty propagation accelerates Bayesian inference in computationally intensive inverse problems. We have shown that using the PCE of model predictions as a surrogate for the forward model significantly reduces the cost of likelihood evaluations, thereby accelerating the solution of the inverse problem using Bayesian inference.

As an application of this method, we have demonstrated three model problems. In the first problem, transient heat flux is estimated in a one-dimensional heat conduction model. The method provides not only a point estimate of the unknown heat flux but also an estimate of the uncertainty bounds in the estimated heat flux. We predicted several profiles of the transient heat flux, which represented varying degrees of smoothness and different scales of transient variation. In the second problem, the method is successfully applied to obtain the solution of the inverse problem to determine the unknown time-dependent heat flux into the disc during a braking process, taking into account the temperature history at some measurement locations. The third problem involves a three-dimensional sounding rocket system to estimate the surface heat flux using temperature measurements inside the rocket shell. The results obtained confirm that the proposed method can accurately estimate the transient heat flux of realistic models irrespective of the size and geometry of the model, and temperature distributions can be obtained using the predicted flux. The proposed method gives accurate estimated values with few measurement data and can be computationally efficient for large and complex models.

The polynomial chaos approach in a Bayesian inference framework could be extended to more complex three-dimensional inverse problems by taking the spatial variation of heat flux. A more advanced form of the proposed methodology can be performed by assuming the correlation time as unknown and predicting it using Bayesian inference. We can infer the correlation time by considering it as an additional hyperparameter. We plan to further explore the framework to study the challenges of spectral uncertainty propagation in spatio-temporal inverse problems.

## Declaration of competing interest

The authors declare that they have no known competing financial interests or personal relationships that could have appeared to influence the work reported in this paper.

## Data availability

No data was used for the research described in the article.

## Acknowledgments

Sufia Khatoon wishes to thank Oil and Natural Gas Corporation (ONGC) India for financial assistance under the Pan IIT-ONGC Collaborative Research Program, India and the Industrial Research and Development (IRD) Unit of Indian Institute of Technology, Delhi, India for providing the financial support.

## References

[1] J.V. Beck, K.J. Arnold, Parameter Estimation in Engineering and Science, John Wiley & Sons, 1977.
[2] O.M. Alifanov, Inverse Heat Transfer Problems, Springer Science & Business Media, 2012.
[3] M.N. Ozisik, Inverse Heat Transfer: Fundamentals and Applications, Crc Press, 2000.
[4] W. Chaze, O. Caballina, G. Castanet, J.-F. Pierson, F. Lemoine, D. Maillet, Heat flux reconstruction by inversion of experimental infrared temperature measurements–Application to the impact of a droplet in the film boiling regime, Int. J. Heat Mass Transfer 128 (2019) 469–478.
[5] J.V. Beck, B. Blackwell, C.R.S. Clair Jr., Inverse Heat Conduction: Ill-Posed Problems, James Beck, 1985.
[6] J. Liu, L.X. Xu, Boundary information based diagnostics on the thermal states of biological bodies, Int. J. Heat Mass Transfer 43 (16) (2000) 2827–2839.
[7] A. M. Djafari, From deterministic to probabilistic approaches to solve inverse problems, in: Bayesian Inference for Inverse Problems, Vol. 3459, International society for optics and photonics, 1998, pp. 2–11.
[8] M.R. Hestenes, E. Stiefel, Methods of conjugate gradients for solving, J. Res. Natl. Bur. Stand. 49 (6) (1952) 409.
[9] T. Abdelhamid, Simultaneous identification of the spatio-temporal dependent heat transfer coefficient and spatially dependent heat flux using an MCGM in a parabolic system, J. Comput. Appl. Math. 328 (2018) 164–176.
[10] K. Levenberg, A method for the solution of certain non-linear problems in least squares, Quart. Appl. Math. 2 (2) (1944) 164–168.
[11] D.W. Marquardt, An algorithm for least-squares estimation of nonlinear parameters, J. Soc. Ind. Appl. Math. 11 (2) (1963) 431–441.
[12] V. Tahmasbi, S. Noori, Inverse identification of temperature-dependent thermal conductivity coefficients in an orthotropic charring composite, Appl. Therm. Eng. 183 (2021) 116219.
[13] M. Singhal, S. Singh, R.K. Singla, K. Goyal, D. Jain, Experimental and computational inverse thermal analysis of transient, non-linear heat flux in circular pin fin with temperature-dependent thermal properties, Appl. Therm. Eng. 168 (2020) 114721.
[14] S. Sun, G. Wang, H. Chen, Application of improved decentralized fuzzy inference methods for estimating the thermal boundary condition of participating medium, Int. J. Therm. Sci. 149 (2020) 106216.
[15] S. Sun, Simultaneous reconstruction of thermal boundary condition and physical properties of participating medium, Int. J. Therm. Sci. 163 (2021) 106853.
[16] M.P. Kaleta, R.G. Hanea, A.W. Heemink, J.D. Jansen, Model-reduced gradient-based history matching, Comput. Geosci. 15 (1) (2011) 135–153.
[17] I. Felde, Estimation of thermal boundary conditions by gradient based and genetic algorythms, in: Materials Science Forum, Vol. 729, Trans Tech Publ, 2013, pp. 144–149.
[18] S. Vakili, M. Gadala, Effectiveness and efficiency of particle swarm optimization technique in inverse heat conduction analysis, Numer. Heat Transfer B 56 (2) (2009) 119–141.
[19] S. Kirkpatrick, C.D. Gelatt, M.P. Vecchi, Optimization by simulated annealing, Science 220 (4598) (1983) 671–680.
[20] Y. Oka, M. Ohno, Parameter estimation for heat transfer analysis during casting processes based on ensemble Kalman filter, Int. J. Heat Mass Transfer 149 (2020) 119232.
[21] S. Khatoon, J. Phirani, S.S. Bahga, Polynomial chaos based solution to inverse problems in petroleum reservoir engineering, in: Fluids Engineering Division Summer Meeting, Vol. 59087, American society of mechanical engineers, 2019, V005T05A076.
[22] F. Zhang, J.A. Skjervheim, A.C. Reynolds, D.S. Oliver, Automatic history matching in a Bayesian framework, example applications, in: SPE Annual Technical Conference and Exhibition, OnePetro, 2003.
[23] J. Wang, N. Zabaras, A Bayesian inference approach to the inverse heat conduction problem, Int. J. Heat Mass Transfer 47 (17–18) (2004) 3927–3941.
[24] P.S. Koutsourelakis, A multi-resolution, non-parametric, Bayesian framework for identification of spatially-varying model parameters, J. Comput. Phys. 228 (17) (2009) 6184–6211.
[25] S. Parthasarathy, C. Balaji, Estimation of parameters in multi-mode heat transfer problems using Bayesian inference-Effect of noise and a priori, Int. J. Heat Mass Transfer 51 (9–10) (2008) 2313–2334.
[26] N. Cao, X. Luo, H. Tang, A Bayesian model to solve a two-dimensional inverse heat transfer problem of gas turbine discs, Appl. Therm. Eng. (2022) 118762.
[27] S. Rana, T. Ertekin, G.R. King, An efficient assisted history matching and uncertainty quantification workflow using Gaussian processes proxy models and variogram based sensitivity analysis: GP-VARS, Comput. Geosci. 114 (2018) 73–83.
[28] A.K. Jha, S.S. Bahga, Uncertainty quantification in modeling of microfluidic T-sensor based diffusion immunoassay, Biomicrofluidics 10 (1) (2016) 014105.
[29] A. Alexanderian, A brief note on the karhunen-loeve expansion, 2015, arXiv preprint arXiv:1509.07526.
[30] Y.M. Marzouk, H.N. Najm, Dimensionality reduction and polynomial chaos acceleration of Bayesian inference in inverse problems, J. Comput. Phys. 228 (6) (2009) 1862–1902.
[31] Y. Efendiev, T. Hou, W. Luo, Preconditioning Markov chain Monte Carlo simulations using coarse-scale models, SIAM J. Sci. Comput. 28 (2) (2006) 776–803.
[32] C. Groetsch, The Theory of Tikhonov Regularization for Fredholm Equations, Boston Pitman Publication, 1984, p. 104.
[33] R. Courant, D. Hilbert, Methods of Mathematical Physics: Partial Differential Equations, Vol. 2, Interscience publishers, 1953.
[34] S. Chib, E. Greenberg, Understanding the metropolis-hastings algorithm, Amer. Statist. 49 (4) (1995) 327–335.
[35] M.T. Reagana, H.N. Najm, R.G. Ghanem, O.M. Knio, Uncertainty quantification in reacting-flow simulations through non-intrusive spectral projection, Combust. Flame 132 (3) (2003) 545–555.
[36] O. Le Maître, O.M. Knio, Spectral Methods for Uncertainty Quantification: With Applications To Computational Fluid Dynamics, Springer Science & Business Media, Berlin, 2010.
[37] S.A. Smolyak, Quadrature and interpolation formulas for tensor products of certain classes of functions, in: Doklady Akademii Nauk, Vol. 148, (5) Russian Academy of Sciences, 1963, pp. 1042–1045.
[38] A. Dąbrowski, L. Dąbrowski, Inverse heat transfer problem solution of sounding rocket using moving window optimization, Plos One 14 (6) (2019) e0218600.